Vibrational Signature of a Single Water Molecule Adsorbed on Pt(111): Towards a Reliable Anharmonic Description

David M. Benoit*

Department of Chemistry, University of Hull, Hull, HU6 7RX, UK

E-mail: d.benoit@hull.ac.uk

Abstract

In this study, we present a thorough benchmarking of our direct anharmonic vibrational variation–perturbation approach for adsorbed molecules on surfaces. We then use our method to describe the vibrational structure of a water molecule adsorbed on a Pt(111) surface and compare our results with the available experimental data. By using an explicitly-correlated hybrid method to describe the molecule–surface interaction, we improve on the initial periodic PBE/DZP potential energy landscape and obtain vibrational frequencies that are of near-experimental accuracy. We introduce an implementation of anharmonic z-polarised IR intensity calculation and explain the absence of antisymmetric O–H stretch in the experimental data for the adsorbed water molecule, while the symmetric O–H stretch is predicted to be visible.

1 Introduction

Adsorbed molecules on metal surfaces are an important part of modern chemistry as they are key to understanding heterogeneous catalysis, electrochemistry, sensing development and the fundamentals of adhesion, to name a few. However, there are still a number of unanswered questions regarding the molecular implications of adsorption, the energetics that decide which site is suitable for a given molecule or the diffusion and reactive kinetics of adsorbed molecules, for example. One of several tools available to surface scientists to answer such questions is vibrational spectroscopy of adsorbed molecules. Indeed, carefully designed experiments can interrogate single or groups of molecules deposited on various surfaces to determine how adsorption alters their properties (see for example Ref.[1]).

In order to understand the vibrational signature of molecules deposited on surfaces and guide experiments, we need to develop theories that go beyond the traditional harmonic regime, as the nature of the interactions at play naturally generate asymmetries in the way the molecule vibrates. Unfortunately, the determination of anharmonic vibrational frequencies for adsorbed molecules on a surface still remains a challenge for both electronic

structure theory and vibrational theory. While model potentials are often used in biological systems with the aid of molecular dynamics simulations, for example, the presence of metal surfaces renders this type of modelling very delicate and a first-principle approach is usually more successful. To date there are only a handful of techniques that are currently able to obtain anharmonic frequencies directly from first principles calculations and even fewer that are able to provide a fully quantum mechanical account of vibrational structure on surfaces.

In this study, we aim to assess the performance of our fast vibrational configuration interaction with perturbation selected interctions (Fast-VCIPSI-PT2) scheme[2] compared to the radial basis function neural network (RBF-NN) approach developed by Manzhos and Carrington.[3] Both approaches can solve the vibrational Schrödinger equation for adsorbed systems. While we have already applied successfully variants of our approach to a number of adsorbed molecular systems (4-mercapto-pyridine on Au(111)[4] and acetylene on Cu(001)[5]), we mainly compared our results to available experimental data. However, in order to truly assess the accuracy of our scheme, it is usefult to compare with theoretical data and thus limit the influence of external factors on the comparison that often occur when using experimental data.

RBF-NN was developed to achieve wavenumber accuracy for low-lying vibrational energy levels by including anharmonicity and high-dimensional mode coupling.[3] Moreover, the approach does not require an analytical representation of the PES and uses instead an automated sampling procedure, suitable to on-the-fly PES construction. It also use a compact set of parametrised Gaussian functions as vibrational basis which is optimised variationally using non-linear fitting. The reported accuracy of RBF-NN (see for example Ref.[6]) and its ability to account for high-dimensional mode coupling make this method a suitable reference for direct vibrational calculations of molecules adsorbed on a surface. Indeed, there are only few published examples of direct calculations of vibrational properties for adsorbed systems. As the study of Manzhos and Carrington[3] uses a potential energy surface computed on-the-fly with the SIESTA periodic density functional theory (DFT) program,[7] this provides a

good benchmark to our direct approach.

The aim of this study is twofold, the first part aims at benchmarking the accuracy of our method in determining vibrational frequencies for adsorbed molecules on surfaces and the second part focuses on developing a methodology that provides reliable predictions of these vibrational frequencies using a hybrid scheme. More specifically, we focus here on the adsorption of a water molecule on Pt(111). There are only very few studies that investigate water monomers on Pt(111)[8,9] and these observations are often hampered by the formation of water clusters or layers as these form quickly on the Pt(111) surface.[10] The formation of water dimers and trimers render the assignment of monomer frequencies difficult, particularly for the O–H stretches.[11] In this study, we selected the two vibrational frequencies that we believe are attributable to a single water molecule adsorbed on the surface. This assignment combines data obtained from single molecule action spectroscopy[8] and more traditional Reflection-Absorption IR Spectroscopy (RAIRS) experiments.[9] We show later on that our calculations are in agreement with this choice.

This paper is organised as follows: we present a summary of our theoretical approach in Section 2, and then provide the computational details of our study in Section 3. Section 4 is divided in two sub-parts: subsection 4.1 discusses how we benchmark our direct VCIPSI-PT2 approach against results obtained in Ref.,[3] first for an isolated water molecule and then for an adsorbed water molecule on Pt(111). In subsection 4.2 we introduce the use of an explicitly-correlated hybrid method to improve of description of adsorbed water and assign observed vibrational modes. Our conclusions are presented in Section 5.

2 Theory

2.1 Vibrational wave function

Throughout this study, we use the VCIPSI-PT2 method to solve the vibrational Schrödinger equation using a potential energy surface (PES) obtained directly from periodic DFT or local

basis set quantum chemical codes (i.e. on the fly construction). The details of our approach can be found elsewhere[2] but we briefly outline the procedure below. The n-dimensional vibrational wave function, $\Psi_{\mathbf{k}}(\mathbf{Q})$, is expressed as a product of single-mode wave functions (modals), $\varphi_i^{(\mathbf{k})}(Q_i)$, in rectilinear normal coordinates, so that:

$$\Psi_{\mathbf{k}}(\mathbf{Q}) = \prod_{i=1}^{n} \varphi_i^{(\mathbf{k})}(Q_i) \tag{1}$$

where $\mathbf{k} = \{k_1, k_2, \ldots, k_n\}$ specifies the excitation quanta of each single-mode wave function.

This leads to a convenient decoupling of the n-dimensional vibrational Schrödinger equation into a set of n independent single mode equations through the introduction of an effective mean-field potential, $\vartheta_i^{(\mathbf{k})}(Q_i)$:

$$\vartheta_i^{(\mathbf{k})}(Q_i) = \left\langle \prod_{j\neq i} \varphi_j^{(\mathbf{k})}(Q_j) \middle| V(\mathbf{Q}) \middle| \prod_{j\neq i} \varphi_j^{(\mathbf{k})}(Q_j) \right\rangle \quad . \tag{2}$$

where $V(\mathbf{Q})$ is the potential energy surface (PES).

Thus we obtain:

$$\left\{ \hat{h}_i(Q_i) + \vartheta_i^{(\mathbf{k})}(Q_i) \right\} \varphi_i^{(\mathbf{k})}(Q_i) = \varepsilon_i^{(\mathbf{k})} \varphi_i^{(\mathbf{k})}(Q_i) \tag{3}$$

where $\hat{h}_i(Q_i) = -\frac{1}{2}\frac{\partial^2}{\partial Q_i^2} + V_i^{(1)}(Q_i)$ is the rectilinear single-mode hamiltonian for mode i. Note that we neglect the Coriolis coupling term in this study as we are mainly interested in pure vibrational spectra. This set of equations is solved self-consistently until convergence of the energy of the vibrational state of interest. This approach is know as the vibrational self-consistent field (VSCF) and has been introduced by Bowman,[12] Carney *et al.*,[13] Cohen *et al.*[14] and Gerber and Ratner.[15]

However, this mean-field approach removes the direct correlation between vibrational modes as each one is treated separately, through the use of $\vartheta_i^{(\mathbf{k})}(Q_i)$. There are a number of methods to recover this correlation such as vibration second-order perturbation the-

ory (VMP2),[16] vibrational configuration interaction (VCI)[17] or vibrational coupled-cluster (VCC),[18] to name a few. Our current approach is based on a variation–perturbation method that combines VCI accuracy but uses multi-reference VMP2 to select the VCI basis iteratively (see Ref.[2] for more details). Once the iterative VCI space is stable, the contribution from the remaining states is included through a perturbative correction.

2.2 Potential energy surfaces

The potential energy for this study is represented using a high-dimensional model, or hierarchical n-mode expansion, of the PES. This approach was suggested by Jung and Gerber[19] for the development of multi-dimensional PES in direct-VSCF calculations. In order to limit the computational effort, the PES is truncated to include only single mode terms, $V_i^{(1)}(Q_i)$, and mode–mode (pairwise) terms, $V_{ij}^{(2)}(Q_i, Q_j)$, so that:

$$V(\mathbf{Q}) = \sum_{i=1}^{n} V_i^{(1)}(Q_i) + \sum_{i=1}^{n} \sum_{j>i}^{n} V_{ij}^{(2)}(Q_i, Q_j) \tag{4}$$

Chaban *et al.*[20] have shown that the pairwise approximation in a VSCF-based approach leads to reasonable vibrational frequencies for large molecular systems. There are a number of advantages to this pairwise representation, in particular it leads naturally to a convenient isomorphism between VSCF equations and standard electronic structure theory, also the scheme offers a practical way of treating large molecular systems since the low-order terms in the expansion are expected to contribute most to the anharmonicity. Finally, the approach also limits the computational effort associated with the construction of the PES to be nominally $O\left(n^2\right)$.

In our implementation,[21] we use a grid approach to compute each terms in the PES, where each point on the grid is computed automatically using density functional theory or quantum chemical methods (direct approach). This approach is convenient as it removes the need for an analytical expression for the $V^n(\mathbf{Q})$ terms. Over the years, we have also

developed a technique that reduces the computational effort further, named fast-VSCF (see Ref.[22–24] for example), and we use this technique in this study to limit the vibrational space to include only the intramolecular modes of the adsorbed water molecule and neglect the explicit coupling between adsorbate and surface. This type of "Born–Oppenheimer" separation of high-frequency and low-frequency modes was chosen to be consistent with the approach of Manzhos and Carrington[3] and also because we showed that the fast-VSCF approach performs well for other adsorbed systems.[4,5]

2.3 Infrared intensities calculations

In order to compute the infrared transition intensities, we construct a global dipole surface expressed as:

$$\vec{\mu}(\mathbf{Q}) = \vec{\mu}(0) + \sum_{i=1}^{n} \vec{\mu}_i(Q_i) \tag{5}$$

where $\vec{\mu}(0)$ is the dipole moment at equilibrium and $\vec{\mu}_i$ is the dipole moment along normal coordinate Q_i. In practice, we compute the dipole moment at each 1D grid point and then interpolate the dipole moment to a finer-meshed representation using a cubic-spline algorithm for each component.

Adapting the formulation of Chaban *et al.*[25] to an uncoupled one-dimensional vibrational wave function for consistency, the strength of the fundamental transition from $\nu_i = 0$ to $\nu_i = 1$ for mode i, I_i, is given by the integral:

$$I_i = \frac{8\pi^3 N_{Av}}{3hc} \nu_i \left| \left\langle \varphi_i^{\nu_i=0}(Q_i) \right| \vec{\mu}_i(Q_i) \left| \varphi_i^{\nu_i=1}(Q_i) \right\rangle \right|^2 \tag{6}$$

where N_{Av} is Avogadro's number, h is Plank's constant, c the speed of light and ν_i is the uncoupled, diagonal, fundamental frequency for mode i. Using this expression, we can also isolate a particular polarisation such as z polarisation for intensities perpendicular to the surface (assuming that the surface normal is parallel to the z direction). The limitation

of the scheme is that it cannot model intensity borrowing or combination bands, as those inherently rely on coupled dipole surfaces.

2.4 Hybrid PES scheme

Our hybrid scheme has already been described in details in a previous study (see Ref.[5] for details), but we present the main features below. The approach is based on an "our own n-layered integrated molecular orbital and molecular mechanics" (ONIOM) type partitioning, where the total energy of the adsorbate molecule is computed using a high-level method, $E(\text{high}, \text{adsorbate})$, and a low-level method, $E(\text{low}, \text{adsorbate})$, then the energy of the entire system (adsorbed molecule and surface) is computed using the same low-level method, $E(\text{low}, \text{system})$.

The total energy of the system is then simply given by:

$$E_{\text{tot}} = E(\text{low}, \text{system}) - E(\text{low}, \text{adsorbate}) + E(\text{high}, \text{adsorbate}). \tag{7}$$

Given that this is an additive scheme, we can use the same approach to compute hybrid dipole moments needed for IR intensities and thus:

$$\vec{\mu}_{\text{tot}} = \vec{\mu}(\text{low}, \text{system}) - \vec{\mu}(\text{low}, \text{adsorbate}) + \vec{\mu}(\text{high}, \text{adsorbate}). \tag{8}$$

As we are mainly investigating water on Pt(111) in this study, there is a clear partitioning between adsorbate and system, without need for any link atoms. A schematic diagram of the partitioning used is shown in Fig. 1.

Our approach gives complete flexibility to use different levels of theory for different parts of the system and allows the use of completely different implementations of electronic structure theory. In this study, the low-level method will be periodic density functional theory (DFT) as our system is periodic, while the high-level method will be explicitly correlated coupled-cluster theory. Note that each level is implemented in a different electronic structure

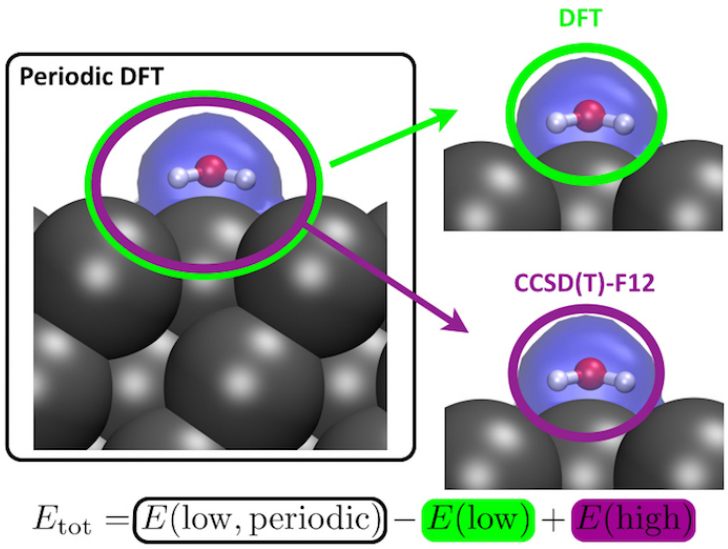

Figure 1: Schematic representation of the hybrid DFT–QM scheme showing the partitioning for a water molecule adsorbed on a Pt(111) surface. See text for details.

package and we use a Python script to compute the final hybrid energy and dipole.

3 Computational details

All periodic density functional calculations use the SIESTA 3.1 program[7] with parameters that follow closely Ref.[3] in order to provide the fairest comparison. We use the Perdew–Burke–Ernzerhof exchange–correlation functional[26] along with a standard double-zeta (DZP) basis set including polarisation functions[27] and corresponding norm-conserving Martins–Troullier pseudo potentials.[28] Those pseudo potentials were initially developed for the ABINIT code[29] but are considered the default pseudo potentials for SIESTA calculations. Following Ref,[3] we use a mesh cutoff and filter cutoff of 400 Ry for both geometry optimisation and force constant calculations. We optimise each wave function with a tolerance on the change in density matrix of 10^{-5}. We also use an increased cutoff radii for the DZP basis (Eshift = 0.01 Rydberg) and $3 \times 3 \times 1$ Monkhorst–Pack k-point mesh to sample the Brillouin zone. The Pt(111) surface is described using a 3 layer model that was kindly provided by the authors of Ref[3] and we relax the topmost layer of Pt while the bottom two layers are

kept fixed at their PBE bulk positions. The unit cell is a 3×3 cell ($a = b = 8.44710$ Å, $\gamma = 60°$) and the separation between the top layer and the bottom layer of the slab image is 15.2 Å which ensures minimal interactions between slabs.

The CCSD(T)-F12 calculations are performed using the ORCA 3.0.2 suite of quantum chemistry programs, using the resolution of the identity approximation (RI-CCSD(T)) along with the cc-pVTZ-F12 basis set,[30] an auxiliary cc-pVTZ-F12-CABS F12 basis set[31] and a cc-pVQZ/C auxiliary basis set for the RI correlation.

We obtain the harmonic normal modes, Q_i, by diagonalising a mass-weighted partial Hessian matrix constructed using force constants computed in SIESTA. Note that all surface atoms are kept frozen during the force constant determination.

The anharmonic vibrational calculations are performed using the VCIPSI-PT2 algorithm[2] implemented in the PVSCF program[21,32] that is developed in our laboratory. We use the *ab initio*/DFT energy values computed for 16 points along each each rectilinear vibrational coordinate to interpolate a finer-meshed representation of the diagonal terms of the PES using a cubic-spline algorithm. The starting and finishing points of each coordinate scan in q-space are optimised to ensure that the curve supports at least eight bound states. Each mode–mode coupling term is computed for 16×16 regularly spaced grid points and then interpolated on a finer mesh using a bicubic interpolation.[33] These points form a discretised version of the PES of the system, $V(\mathbf{Q})$, as formulated in Eq. (4).

All the 1-D VSCF equations are solved using the FGH method.[34,35] We compute the correlation corrections using the VCIPSI-PT2 method and explore a VCI basis made of all one-mode, two-mode and three-mode excitations (VCISDT) up to seven excitation quanta ($n_{\max} = 7$). The iterative VCI matrices are diagonalised using our own implementation of the Davidson algorithm. Note that the vibrational calculation is only performed for the Γ-point of the Brillouin zone (Γ approximation[4,36]).

The anharmonic transition intensities are computed using a diagonal (1D) representation of the dipole surface and the 1D vibrational wave functions (i.e. without including effects

from vibrational correlation).

4 Results

4.1 Benchmarking our approach

For our benchmarking we use SIESTA along with a Pt(111) surface model and parameters set (kindly provided by the authors of Ref.[3]) to perform direct Fast-VCIPSI-PT2 calculations on an adsorbed water molecule on Pt(111). Note that there could be small differences between the SIESTA version and parameters that we use and those of Ref.,[3] but these are considered suitably small to be nearly identical in both cases. As both approaches compute essentially exact solutions to the vibrational Schrödinger equation, we expect that differences in computed vibrational frequencies can be mainly attributed to the description of mode–mode couplings (2-D PES for our approach vs 3-D PES for RBF-NN).

4.1.1 Isolated water molecule

The vibrational spectrum of an isolated water molecule provides an initial simpler benchmark of our implementation compared to the RBF-NN approach. The spectrum of the water molecule was computed in Ref.[3] as it was used in order to compute the vibrational shift caused by adsorption on a Pt(111) surface.

Before computing the vibrational spectrum, we first optimise the water molecule geometry at the PBE/DZP level of theory and obtain d(O–H) = 0.972 Å and ∠(H–O–H) = 104.5°, in agreement with the results reported in Ref.[3] (d(O–H) = 0.97 Å and ∠(H–O–H) = 104.3°). Using the optimised geometry, we compute the Hessian matrix and then use the normal modes to construct the necessary PES for the anharmonic calculation. Our VCIPSI-PT2 results are shown in Table 1, where we use two types of PES for water: one constructed using SIESTA and parameters identical to those used for the adsorbed water molecule on Pt(111) and a more accurate RI-CCSD(T)-F12/cc-pVTZ-F12 PES obtained with ORCA. Note that

we include coupling between all mode pairs.

Table 1: Comparison of the fundamental vibrational frequencies of the water molecule computed using the VCIPSI-PT2 method and the RBF-NN approach. All frequencies are in cm^{-1} and the relative IR transition intensities are given in parentheses. Note that the PBE PES is computed using SIESTA at the PBE/DZP level of theory and that the RI-CCSD(T)-F12 results are computed using ORCA and a cc-pVTZ-F12 basis set. The IR transition intensities are computed using a 1D representation only.

Mode	RBF-NN[3]	VCIPSI-PT2			
PES	PBE	PBE	RI-CCSD(T)-F12	Exp.[37](Intens.[38])	
1	3600	3576 (1.00)	3738 (0.73)	3756 (0.60)	ν_3 (B2)
2	3468	3444 (0.006)	3642 (0.004)	3657 (0.03)	ν_1 (A1)
3	1525	1537 (0.79)	1603 (1.00)	1595 (1.00)	ν_2 (A1)
rms dev.	—	21	136	147	
rms dev.	147	165	14	—	

We see that our results are in good agreement with the RBF-NN results from Ref.,[3] with the largest deviations occurring for both stretching modes (24 cm^{-1} difference for each mode). We note that the overall rms deviation is only 21 cm^{-1}, a reasonable result given that we neglect the mode–mode–mode (3D) coupling in our water PES whereas it is implicitly included in the RBF-NN results. In a previous study of methanol,[39] we quantified the accuracy loss caused by limiting the PES expansion to 2D coupling to about 30 cm^{-1}. Indeed, if we express the PES in curvilinear normal coordinates using this approach —which tends to improve the 2D description of the PES (see below)— the VCIPSI-PT2 method leads to $\nu_3 = 3615$ cm^{-1}, $\nu_1 = 3470$ cm^{-1} and $\nu_2 = 1543$ cm^{-1} and a lower rms deviation of 13 cm^{-1} from the RBF-NN values. It should also be noted that the differences in versions of SIESTA and calculation parameters could also lead to deviations of a similar order of magnitude.

If we now focus on the measured fundamental frequencies reported in Table 1, we observe that the vibrational results obtained using a PBE/DZP PES and either vibrational method show a marked deviation for both stretching modes (over 200 cm^{-1} for the symmetric stretch

ν_1) resulting in a rms deviation of 147 cm^{-1} for RBF-NN and 165 cm^{-1} for VCIPSI-PT2. Note that the bending mode is reasonably well reproduced, with deviations of 70 cm^{-1} and 58 cm^{-1} for RBF-NN and VCIPSI-PT2, respectively. This is consistent with the observation that bond stretches are often too weak in DFT while bending modes are better described by this approach.[4]

Using a wave function based approach, such as the RI-CCSD(T)-F12/cc-pVTZ-F12, to compute the PES offers a much better description of the vibrational spectrum of water. We see that the maximum error for this PES using the VCIPSI-PT2 approach is now 18 cm^{-1} for the asymmetric stretch (ν_3) and the overall rms deviation is lowered to 14 cm^{-1}, an order of magnitude more accurate. The remaining error can be attributed to the lack of 3D couplings in the PES and neglected rotation–vibration terms in the Hamiltonian, which can amount up to 13 cm^{-1} for water (see Ref.[40]). In support of this assumption, a VCIPSI-PT2 calculation using the same PES but expressed in curvilinear normal coordinates leads to $\nu_3 = 3758$ cm^{-1}, $\nu_1 = 3662$ cm^{-1} and $\nu_2 = 1599$ cm^{-1} and thus a rms deviation of merely 4 cm^{-1} from the experimental values. We have shown that such coordinate transformation leads to a much improved description of the vibrational problem,[39] nearly eliminating the need for 3D couplings in some systems.

Finally, let's consider the IR transition intensities for each mode as shown in parentheses in Table 1. This quantity was not reported in the study of Manzhos and Carrington,[3] so we cannot compare with their results. However, experimental values do exist and these are reported in the last column of Table 1. First of all, we note that both dipole surfaces (PBE and CCSD(T)-F12) predict that the totally symmetric ν_1 mode is of very low intensity, in accordance with the available experimental data. However, while the asymmetric stretch (ν_3) and the bending mode (ν_2) are predicted to be intense for both PES, we note that the dipole surface obtained from PBE calculations predicts the asymmetric stretch to be the most intense, while CCSD(T)-F12 correctly assigns the most intense transition to the bending mode, in accordance with experimental data. This could indicate that the PBE/DZP dipole

moment is only qualitatively reliable, i.e. it can be used to predict if a mode is not IR active, but might be less reliable when predicting intensity patterns.

4.1.2 Geometry and energetics of H_2O on Pt(111)

The water molecule adsorbs preferentially on a top site of the Pt(111) surface, as remarked by a number of studies (see Ref.[41] for an overview). The internal geometry of the water molecule changes slightly to longer bond lengths, d(O–H) = 0.987 Å, and a slightly more acute H–O–H angle, ∠(H–O–H) = 103.2°, in full agreement with Ref.[3] If we now consider the inter-molecular degrees of freedom, the distance between the oxygen atom of water and the nearest Pt atom is d(O–Pt) = 2.53 Å and the average water tilt angle ∠(H–O–Pt) = 87.7°. This is longer than the result of d(O–Pt) = 2.31 Å reported in Ref.,[3] but longer distances have also been reported for the monomer (for example, d(O–Pt) = 2.40 Å in Ref.[41]).

We also computed the adsorption energy of water on the top site of Pt(111) by subtracting the total energy of the relaxed water molecule and relaxed bare Pt(111) surface from that of the adsorbed water on Pt(111). Our results, $E_{\text{ads.}}^{\text{PBE}} = E_{\text{opt}}^{\text{PBE}}(\text{H}_2\text{O@Pt(111)}) - E_{\text{opt}}^{\text{PBE}}(\text{H}_2\text{O}) - E_{\text{opt}}^{\text{PBE}}(\text{Pt(111)}) = -60.8$ kJ/mol (or -0.63 eV) is slightly smaller than the adsorption energy determined in Ref.[3] The current experimental estimate of the dissociation energy[42] is obtained from calorimetry for D_2O on Pt(111) and is $E_{\text{ads.}}^{\text{exp.}} = -51.3 \pm 1.6$ kJ/mol, which is in good agreement with our value. Earlier measurements are also available, for example $E_{\text{ads.}}^{\text{exp.}} = -54.2 \pm 3$ kJ/mol was obtained by examination of adsorption kinetics[10] and $E_{\text{ads.}}^{\text{exp.}} = -52 \pm 2$ kJ/mol from temperature-programmed desorption.[43] However, despite the good agreement, note that these measurements are not specifically performed on single molecules and are likely to include collective effects originating from neighbouring molecules. Indeed, Meng *et al.*[41] have reported binding energies for water clusters and water bilayers on Pt(111) that would indicate that collective effects can have a significant influence on the binding energy (up to 70% increase in adsorption energy per water molecule).

4.1.3 Benchmarking vibrational frequencies for H_2O on Pt(111)

Similarly to the isolated water molecule, we use the optimised geometry of the adsorbed water molecule on the top site of Pt(111) obtained at the PBE/DZP level of theory and compute a partial Hessian matrix where all Pt atoms are considered fixed. This Hessian matrix contains 3 internal degrees of freedom (3 water modes) and 6 "inter-molecular" modes that describe the frustrated translation of H_2O on the surface and the rotation of the molecule above the surface. As Ref.[3] only considered the internal modes of the water molecule, we use our Fast-VSCF technique to limit our VCIPSI-PT2 calculation to only account for those 3 modes, with couplings up to 2D, while neglecting all inter-molecular modes in a first instance. The results of our vibrational calculations are summarised in Table 2, along with those of Ref.[3] for comparison.

Table 2: Computed fundamental vibrational frequencies of a water molecule adsorbed on a Pt(111) surface. Comparison between the VCIPSI-PT2 method and the RBF-NN approach both without and with mode couplings. All frequencies are in cm^{-1}. Note that the PBE PES is computed using SIESTA and the PBE/DZP level of theory.

	1D PES		Coupled PES		
Mode	RBF-NN[3]	Diagonal	RBF-NN	Fast-VCIPSI-PT2	
1	3561	3608	3216	3264	$\nu_{\text{anti.}}$
2	3235	3294	3119	3175	$\nu_{\text{sym.}}$
3	1510	1521	1452	1465	ν_{bend}
rms dev.	–	44	–	43	

In order to mitigate the different treatment of mode–mode coupling between the RBF-NN approach and our VCIPSI-PT2 method, we first compare the results obtained using a PES limited to a sum of 1D terms (first two results columns of Table 2). We observe that both methods lead to similar results, with the symmetric stretch showing the largest deviation (59 cm^{-1}), followed by the antisymmetric stretch (47 cm^{-1}) and finally the best agreement is obtained for the bending mode with only 11 cm^{-1} deviation from the benchmark data of Ref.[3]

If we now include up to 2D intramolecular coupling for water (see last two results columns of Table 2), keeping in mind that RBF-NN implicitly couples all 3 modes together, we see that our results remain of similar quality, with deviations of a similar order — larger for $\nu_{\text{sym.}}$ (56 cm^{-1}) than for $\nu_{\text{anti.}}$ (48 cm^{-1}) and the best agreement between the two methods for ν_{bend} (13 cm^{-1}). This is in line with our observation for the isolated water molecule, where our computed bending mode frequency seem to be in better agreement with RBF-NN than the O–H stretches. One other interesting point is the fact that either of our 1D and 2D models lead to anharmonic frequencies that are higher than those computed using the RBF-NN approach. This could be indicative of a systematic issue in either approaches.

To summarise, we see that the VCIPSI-PT2 approach provides results that are of similar quality to those obtained using the RBF-NN method developed by Manzhos and Carrington[3] and we are confident that both approaches are congruent. We computed an rms deviation of about 20 cm^{-1} for the fundamental frequencies of an isolated water molecule and about 45 cm^{-1} for those of H_2O on Pt(111), which is coherent with the error caused by neglecting mode–mode couplings higher than 2D. Unfortunately, our current curvilinear implementation is not applicable to molecules on surfaces and thus we will use exclusively rectilinear coordinates for adsorbed systems. Finally, it is worth noting that the error of typical surface spectroscopy measurements (HREELS or action spectroscopy,[8] for example) can be of the order of several meV (tens of cm^{-1}) and thus the difference observed between our approach and that of Ref.[3] is commensurate with the experimental error.

4.2 Improving the description of adsorbed water on Pt(111)

Having now benchmarked the results of our VCIPSI-PT2 approach for water adsorbed on Pt(111), we now investigate how realistic the SIESTA PBE/DZP approach is at describing the vibrational experimental data. Table 3 presents a comparison of the fundamental vibrational frequencies (along with z-polarised IR intensities) of a single water molecule adsorbed on a top site of Pt(111) compared to the available experimental data. Note that we use

our Fast-VSCF technique to limit the VCIPSI-PT2 calculation to only account for the three intra-molecular water modes ($\nu_{\text{anti.}}$, $\nu_{\text{sym.}}$, ν_{bend}), with couplings up to 2D, while neglecting all adsorbate–surface modes (translation and rotation of the water molecule above the surface) and all Pt(111) phonons.

Table 3: Water adsorbed on a Pt(111) surface – hybrid results. Note that the PBE PES is computed using SIESTA at the PBE/DZP level of theory and that the RI-CCSD(T)-F12 results are computed using ORCA and a cc-pVTZ-F12 basis set. The z-polarised IR transition intensities are computed using a 1D representation only. D3 corrections are BJ-damped Grimme corrections using the dftd3 program and applied *a posteriori*.

	VCIPSI-PT2				
Mode	PBE	PBE-D3	CCSD(T)-F12‖PBE-D3	Exp	
1	3264 (0.004)	3255 (0.004)	3438 (0.004)	—	$\nu_{\text{anti.}}$
2	3175 (0.73)	3166 (0.73)	3385 (0.47)	3344 ± 8 Ref.[9]	$\nu_{\text{sym.}}$
3	1465 (1.00)	1466 (1.00)	1532 (1.00)	1550 ± 20 Ref.[8]	ν_{bend}
rms dev.	133	139	31	–	

If we consider the first result column of Table 3, which compares our VCIPSI-PT2 results obtained for a standard PBE/DZP PES using SIESTA, we note that there is a significant deviation from experimental results. The symmetric stretch $\nu_{\text{sym.}}$ shows a very large deviation of 169 cm^{-1} and the bending mode a slightly smaller deviation of 85 cm^{-1}. The antisymmetric stretching mode is unlikely to be visible due to negligible z-polarised IR intensity. We compute a large rms deviation of 133 cm^{-1} for the combination of the two visible frequencies, with both predicted fundamentals underestimating the experimental data. We also observed this type of poor agreement for anharmonic frequencies obtained from a PES constructed using the PBE exchange–correlation functional in our investigation of acetylene on Cu(001)[5] for a number of stretching and bending modes.

There has been a recent interest in correcting DFT approaches to include dispersion forces for adsorbed molecules[44,45] as these can have an impact on binding energies, adsorbate–surface distances and possibly vibrational frequencies. In order to investigate the role of dispersion in this system, we use the DFT-D3 approach suggested by Grimme[44] (including their

Becke–Johnson finite-damping term[46]) as implemented in their dftd3 program V3.1 (available from Grimme's website) and add this as an *a posteriori* correction to our PBE/DZP potential energy surface. This means that a D3 correction is computed for every point on our PES and added to the existing energy values obtained from SIESTA. Note that we also include contributions from Axilrod–Teller–Muto three-centre dispersion terms to the standard D3 dispersion energy correction. These three-body correction terms (denoted D3(ABC) in the literature) account for the non-pairwise additivity of the dispersion terms[44] and have been shown to be significant for adsorbed molecules.[47] The corresponding anharmonic vibrational results are shown in the second result column of Table 3. As this procedure has no effect on the dipole moment of the system, the z-polarised IR intensities are the same as those obtained with the original PBE/DZP surface.

We observe that dispersion corrections do not influence the anharmonic frequencies much in this case, with the largest deviation occurring for both O–H stretching modes (9 cm^{-1} difference) and only 1 cm^{-1} difference for the bending mode. Both stretching modes are thus slightly weakened by the addition of a dispersion term while the bending mode remains unaffected — this is not unexpected as this system is unlikely to display large changes in dispersion effects during intramolecular vibrations. However, the binding energy of the water molecule on the top site of Pt(111) is more strongly affected by dispersion corrections, leading to a corrected adsorption energy of $E_{\mathrm{ads.}}^{\mathrm{PBE-D3}} = -78.2$ kJ/mol (or -0.81 eV), including three-body corrections.

Since we are focusing on the fundamental internal vibrations of the adsorbed monomer on the surface rather than on its frustrated translations and rotations, we can use a hybrid scheme to improve the quality of the intramolecular PES. The approach we developed recently for the vibrations of acetylene on Cu(001)[5] can be easily applied here by constructing a hybrid PES where the water molecule is described at the RI-CCSD(T)-F12/cc-pVTZ-F12 level of theory while the rest of the system is computed using periodic PBE-D3/DZP calculations. Indeed, we have shown for the isolated water molecule in Section 4.1.1 that

CCSD(T)-F12 leads to anharmonic frequencies and IR intensities that are in very good agreement with the available experimental data. Therefore, "merging" both techniques using a hybrid scheme should offer a better description of the internal degrees of freedom of water, while retaining the periodic description of the metal surface.

The results obtained with our hybrid PES are shown in the third result column of Table 3. We see immediately that using a high-level correlation method for the water PES improves significantly the agreement with experiment. The O–H stretch frequencies increase by 183 cm^{-1} ($\nu_{anti.}$) and 219 cm^{-1} ($\nu_{sym.}$), while ν_{bend} increases by 66 cm^{-1}. Such mode stiffening is characteristic of the difference between PBE and explicitly-correlated methods and is already apparent for the isolated water molecule results shown in Table 1, for example. For the adsorbed water molecule on Pt(111), this PES improvement leads to a dramatic reduction of the deviation from the available experimental data with only 41 cm^{-1} difference for the symmetric stretch ($\nu_{sym.}$) and 18 cm^{-1} for the bending mode (ν_{bend}). The rms deviation for our hybrid approach from the measured vibrational fundamentals is 31 cm^{-1} (or 4 meV), within the accepted experimental error for this type of surface measurements (see also error bars in Table 3).

Interestingly, removing the D3 dispersion corrections from our hybrid PES (i.e. using standard PBE/DZP for the periodic system instead) does not affect the vibrational results much. We see the bending frequency left unchanged at $\nu_{bend} = 1532$ cm^{-1}, while there is a very small increase for both O–H stretching frequencies ($\nu_{anti.} = 3444$ cm^{-1} and $\nu_{sym.} = 3389$ cm^{-1}). Overall the rms deviation from the measured vibrational fundamentals is slightly higher (34 cm^{-1}) compared to the results of the dispersion-corrected hybrid shown in Table 3. This highlights that the explicitly-correlated part of the hybrid PES (CCSD(T)-F12) corrects the intramolecular region, which is the main part of the PES probed by the experimental data, but that dispersion corrections do not impact the frequencies of the water molecule much, as seen earlier for pure PBE vs PBE-D3 PES.

Let's consider the z-polarised IR intensities reported in Table 3. We see that for both

DFT and hybrid dipole models, the antisymmetric mode ($\nu_{\text{anti.}}$) has a very low intensity compared to that of the other two modes, rendering it nearly invisible to techniques for which the selection rule requires a dipole change perpendicular to the surface. This is the case for a number of surface spectroscopies, such as RAIRS or EELS,[48] and thus we predict that $\nu_{\text{anti.}}$ is unlikely to be observed using standard surface techniques. The bending mode (ν_{bend}) is predicted to be the most intense by both PBE and hybrid dipole surfaces, and the symmetric stretch ($\nu_{\text{sym.}}$) is now predicted to be visible, albeit with a disagreement in relative intensity between PBE and hybrid PES.

5 Conclusions

In this study, we have benchmarked our direct VCIPSI-PT2 approach with vibrational results obtained with a different method (fully-coupled RBF-NN[3]) but for a PES computed using the same periodic DFT program (SIESTA). We compared results obtained for an isolated water molecule and a water molecule adsorbed on the top site of a Pt(111) surface and found our results to be in agreement with the RBF-NN results, if we account for possible differences in SIESTA versions and absence of mode–mode coupling involving more than two modes in our approach. In all cases, our approach has proven to be of sufficient accuracy to compare to available surface spectroscopy data.

We also presented our implementation of z-polarised IR intensities calculation, which is necessary for the understanding of surface vibrational data. Indeed, a number of common surface science techniques have propensity rules that disallow signal from vibrations without dipole change perpendicular to the surface (z direction in our case). Using our method we showed for a water molecule adsorbed on Pt(111) that the antisymmetric mode ($\nu_{\text{anti.}}$) has a very low intensity but that the symmetric mode ($\nu_{\text{sym.}}$) and the bending modes (ν_{bend}) are intense. This is in contrast with the IR spectrum of the isolated water molecule, for which both theory and experiment agree that its symmetric mode (ν_1) has a low IR inten-

sity. Therefore, it appears that the IR signal from a water molecule is deeply affected by attachment on a Pt(111) surface. This is mainly due to the geometry at the binding site (top site in this case) and the electronic redistribution that occurs upon binding.

We noted that *a posteriori* dispersion correction (PBE-D3) affects the adsorbate–surface binding energy more that the adsorbate internal vibrational spectrum, causing only marginal changes in vibrational structure. However, these corrections (including three-body terms) are not sufficient to improve the vibrational description of the water monomer attached to the Pt(111) surface. It can be concluded in this case that dispersion corrections most likely shift the entire PES to lower energies (explaining the increased binding energy) but that the dispersion-corrected PES retains the original curvature obtained from uncorrected PBE/DZP.

Finally, we also showed that it is possible to achieve a very accurate description of the water vibrational spectrum by using a hybrid QM-DFT approach. The use of explicitly-correlated CCSD(T)-F12 to describe the water molecule within a hybrid scheme for the computation of PES of adsorbed molecules leads to dramatic improvements in the predicted vibrational spectrum and enables us to obtain near-experimental accuracy for this system. In particular, this also enables us to identify the vibrations originating from the water monomer on the surface — a task that has thus far remained difficult experimentally due to the natural tendency of water to cluster together on the surface.

Our new benchmarked approach is thus suitable to exploring further the vibrational behaviour of adsorbates on surfaces by providing a solid quantum mechanical treatment of both vibrational structure and vibrational intensities. This work also highlights the importance of a reliable description of the potential energy surface beyond standard DFT approaches. Such description is achieved here by using a hybrid methodology that combines periodic DFT with advanced explicitly-correlated quantum chemical techniques.

Acknowledgement

This work has been partly funded by the University of Hull and partly by a Marie Curie International Research Staff Exchange Scheme Fellowship within the 7th European Community Framework Programme under Grant No. IRSES-GA-2012-31754. We also thank D. Lauvergnat, S. Manzhos and T. Carrington Jr. for helpful discussions.

References

(1) Chiang, C.; Xu, C.; Han, Z.; Ho, W. Real-space imaging of molecular structure and chemical bonding by single-molecule inelastic tunneling probe. *Science.* **2014**, *344*, 885–888.

(2) Scribano, Y.; Benoit, D. M. Iterative active-space selection for vibrational configuration interaction calculations using a reduced-coupling VSCF basis. *Chem. Phys. Lett.* **2008**, *458*, 384–387.

(3) Manzhos, S.; Carrington Jr., T.; Yamashita, K. Calculating anharmonic vibrational frequencies of molecules adsorbed on surfaces directly from ab initio energies with a molecule-independent method: H_2O on Pt(111). *Surface Science* **2011**, *605*, 616–622.

(4) Ulusoy, I. S.; Scribano, Y.; Benoit, D. M.; Tschetschetkin, A.; Maurer, N.; Koslowski, B.; Ziemann, P. Vibrations of a single adsorbed organic molecule: anharmonicity matters. *Phys. Chem. Chem. Phys.* **2011**, *13*, 612–618.

(5) Chulkov, S. K.; Benoit, D. M. A fragment method for systematic improvement of anharmonic adsorbate vibrational frequencies: Acetylene on Cu(001). *J. Chem. Phys.* **2013**, *139*, 214704–1–214704–8.

(6) Manzhos, S.; Yamashita, K.; Carrington Jr., T. Using a neural network based method

to solve the vibrational Schrödinger equation for H_2O. *Chem. Phys. Lett.* **2009**, *474*, 217–221.

(7) Soler, J. M.; Artacho, E.; Gale, J. D.; Garca, A.; Junquera, J.; Ordejón, P.; Sánchez-Portal, D. The SIESTA method for ab initio order-N materials simulation. *J. Phys.: Condens. Matter* **2002**, *14*, 2745–2779.

(8) Motobayashi, K.; Árnadóttir, L.; Matsumoto, C.; Stuve, E. M.; Jónsson, H.; Kim, Y.; Kawai, M. Adsorption of water dimer on platinum(111): Identification of the –OH $\cdots$ Pt hydrogen bond. *ACS Nano* **2014**, *8*, 11583–11590.

(9) Ogasawara, H.; Yoshinobu, J.; Kawai, M. Water adsorption on Pt(111): from isolated molecule to three-dimensional cluster. *Chem. Phys. Lett.* **1994**, *231*, 188–192.

(10) Daschbach, J. L.; Peden, B. M.; Smith, R. S.; Kay, B. D. Adsorption, desorption, and clustering of H_2O on Pt(111). *J. Chem. Phys.* **2004**, *120*, 1516–1523.

(11) Jacobi, K.; Bedürftig, K.; Wang, Y.; Ertl, G. From monomers to ice — new vibrational characteristics of H_2O adsorbed on Pt(111). *Surface Science* **2001**, *472*, 9–20.

(12) Bowman, J. M. Self-consistent field energies and wave functions for coupled oscillators. *J. Chem. Phys.* **1978**, *68*, 608–610.

(13) Carney, G. C.; Sprandel, L. L.; Kern, C. W. Variational approaches to vibration-rotation spectroscopy for polyatomic molecules. *Adv. Chem. Phys.* **1978**, *37*, 305–379.

(14) Cohen, M.; Greita, S.; McEarchran, R. P. Approximate and exact quantum mechanical energies and eigenfunctions for a system of coupled oscillators. *Chem. Phys. Lett.* **1979**, *60*, 445–450.

(15) Gerber, R. B.; Ratner, M. A. A semiclassical self-consistent field (SC SCF) approximation for eigenvalues of coupled-vibration systems. *Chem. Phys. Lett.* **1979**, *68*, 195–198.

(16) Christiansen, O. Møller–Plesset perturbation theory for vibrational wave functions. *J. Chem. Phys.* **2003**, *119*, 5773–5781.

(17) Christoffel, K. M.; Bowman, J. M. Investigations of self-consistent field, SCF CI and virtual state configuration-interaction vibrational energies for a model three-mode system. *Chem. Phys. Lett.* **1982**, *85*, 220–224.

(18) Christiansen, O. Vibrational coupled cluster theory. *J. Chem. Phys.* **2004**, *120*, 2149–2159.

(19) Jung, J. O.; Gerber, R. B. Vibrational wave functions and spectroscopy of $(H_2O)_n$, $n = 2, 3, 4, 5$: Vibrational self-consistent field with correlation corrections. *J. Chem. Phys.* **1996**, *105*, 10332–10348.

(20) Chaban, G. M.; Jung, J. O.; Gerber, R. B. Ab initio calculation of anharmonic vibrational states of polyatomic systems: Electronic structure combined with vibrational self-consistent field. *J. Chem. Phys.* **1999**, *111*, 1823–1829.

(21) Benoit, D. M.; Madebene, B.; Ulusoy, I.; Mancera, L.; Scribano, Y.; Chulkov, S. Towards a scalable and accurate quantum approach for describing vibrations of molecule–metal interfaces. *Beilstein J. Nanotechnol.* **2011**, *2*, 427–447.

(22) Benoit, D. M. Fast vibrational self-consistent field calculations through a reduced mode–mode coupling scheme. *J. Chem. Phys.* **2004**, *120*, 562–573.

(23) Benoit, D. M. Efficient correlation-corrected vibrational self-consistent field computation of OH-stretch frequencies using a low-scaling algorithm. *J. Chem. Phys.* **2006**, *125*, 244110–1–244110–7.

(24) Benoit, D. M. Fast vibrational calculation of anharmonic OH-stretch frequencies for two low-energy noradrenaline conformers. *J. Chem. Phys.* **2008**, *129*, 234304–1–234304–9.

(25) Chaban, G. M.; Jung, J. O.; Gerber, R. B. Anharmonic vibrational spectroscopy of glycine: testing of ab initio and empirical Potentials. *J. Phys. Chem. A* **2000**, *104*, 10035–10044.

(26) Perdew, J. P.; Burke, K.; Ernzerhof, M. Generalized gradient approximation made simple. *Phys. Rev. Lett.* **1996**, *77*, 3865–3868.

(27) Junquera, J.; Paz, O.; Sánchez-Portal, D.; Artacho, E. Numerical atomic orbitals for linear-scaling calculations. *Phys. Rev. B.* **2001**, *64*, 235111–1–235111–9.

(28) Troullier, N.; Martins, J. L. Efficient pseudopotentials for plane-wave calculations. *Phys. Rev. B.* **1991**, *43*, 1993–2006.

(29) ABINIT code. `http://www.abinit.org`, Accessed: 2015-11-02.

(30) Peterson, K. A.; Adler, T. B.; Werner, H.-J. Systematically convergent basis sets for explicitly correlated wavefunctions: The atoms H, He, B-Ne, and Al-Ar. *J. Chem. Phys.* **2008**, *128*, 084102–1–84102–12.

(31) Yousaf, K. E.; Peterson, K. A. Optimized auxiliary basis sets for explicitly correlated methods. *J. Chem. Phys.* **2008**, *129*, 184108–1–184108–7.

(32) PVSCF code. `http://www.pvscf.org`, Accessed: 2015-11-02.

(33) Akima, H. Algorithm 760: Rectangular-grid-data surface fitting that has the accuracy of a bicubic polynomial. *ACM Transactions on Mathematical Software* **1996**, *22*, 357–361.

(34) Martson, C. C.; Balint-Kurti, G. G. The Fourier grid Hamiltonian method for bound state eigenvalues and eigenfunctions. *J. Chem. Phys.* **1989**, *91*, 3571–3576.

(35) Balint-Kurti, G. G.; Ward, C. L.; Martson, C. C. Two computer programs for solving the Schrödinger equation for bound-state eigenvalues and eigenfunctions using the Fourier grid Hamiltonian method. *Comp. Phys. Commun.* **1991**, *67*, 285–292.

(36) Keçeli, M.; Hirata, S.; Yagi, K. First-principles calculations on anharmonic vibrational frequencies of polyethylene and polyacetylene in the Γ approximation. *J. Chem. Phys.* **2010**, *133*, 034110–1–034110–6.

(37) Benedict, W. S.; Gailar, N.; Plyler, E. K. Rotation-vibration spectra of deuterated water vapor. *J. Chem. Phys.* **1956**, *24*, 1139–1165.

(38) Camy-Peyret, C.; Flaud, J.-M. Vibration–rotation dipole moment operator for asymmetric rotors. In *Molecular Spectroscopy: Modern Research, Volume 3*; Rao, K., Ed.; Elsevier, 1985; pp 69 – 110.

(39) Scribano, Y.; Lauvergnat, D. M.; Benoit, D. M. Fast vibrational configuration interaction using generalized curvilinear coordinates and self-consistent basis. *J. Chem. Phys.* **2010**, *133*, 094103–1–094103–12.

(40) Carbonniere, P.; Barone, V. Coriolis couplings in variational computations of vibrational spectra beyond the harmonic approximation: implementation and validation. *Chem. Phys. Lett.* **2004**, *392*, 365–371.

(41) Meng, S.; Wang, E. G.; Gao, S. Water adsorption on metal surfaces: A general picture from density functional theory studies. *Phys. Rev. B.* **2004**, *69*, 195404–1–195404–13.

(42) Lew, W.; Crowe, M. C.; Karp, E.; Campbell, C. T. Energy of molecularly adsorbed water on clean Pt(111) and Pt(111) with coadsorbed oxygen by calorimetry. *J. Phys. Chem. C* **2011**, *115*, 9164–9170.

(43) Haq, S.; Harnett, J.; Hodgson, A. Growth of thin crystalline ice films on Pt(111). *Surface Science* **2002**, *505*, 171–182.

(44) Grimme, S.; Antony, J.; Ehrlich, S.; Krieg, H. A consistent and accurate ab initio parametrization of density functional dispersion correction (DFT-D) for the 94 elements H-Pu. *J. Chem. Phys.* **2010**, *132*, 154104–1–154104–19.

(45) Lee, K.; Berland, K.; Yoon, M.; Andersson, S.; Schröder, E.; Hyldgaard, P.; Lundqvist, B. I. Benchmarking van der Waals density functionals with experimental data: potential-energy curves for H_2 molecules on Cu(111), (100) and (110) surfaces. *J. Phys.: Condens. Matter* **2012**, *24*, 424213–1–424213–15.

(46) Grimme, S.; Ehrlich, S.; Goerigk, L. Effect of the damping function in dispersion corrected density functional theory. *J. Comput. Chem.* **2011**, *32*, 1456–1465.

(47) Reckien, W.; Eggers, M.; Bredow, T. Theoretical study of the adsorption of benzene on coinage metals. *Beilstein J. Org. Chem.* **2014**, *10*, 1775–1784.

(48) Sebastian, K. L. The selection rule in electron energy loss spectroscopy of adsorbed molecules. *J. Phys. C: Solid St. Phys.* **1980**, *13*, L115–L117.

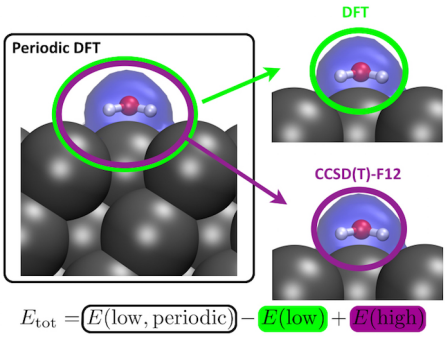
Periodic DFT
DFT
CCSD(T)-F12
$E_{\mathrm{tot}} = E(\mathrm{low, periodic}) - E(\mathrm{low}) + E(\mathrm{high})$